Available online at www.sciencedirect.com
SCIENCE DIRECT®
European Journal of Pharmacology 491 (2004) 9–19
www.elsevier.com/locate/ejphar

Pharmacological analysis and molecular cloning of the canine equilibrative nucleoside transporter 1

James R. Hammond*, Meaghan Stolk, Richard G.E. Archer, Kristy McConnell

Department of Physiology and Pharmacology, M216 Medical Sciences Building, University of Western Ontario, London, Ontario, Canada N6A 5C1

Received 10 November 2003; received in revised form 4 March 2004; accepted 10 March 2004

Abstract

We studied the binding of [^{3}H]nitrobenzylthioinosine (NBMPR) and the uptake of [^{3}H]formycin B by the *es* (equilibrative inhibitor-sensitive) nucleoside transporter of Madin Darby Canine Kidney (MDCK) cells. NBMPR inhibited [^{3}H]formycin B uptake with a K_i of 2.7 ± 0.6 nM, and [^{3}H]NBMPR had a K_D of 1.3 ± 0.3 nM for binding to these cells; these values are significantly higher than those obtained in human and mouse cell models. In contrast, other recognized *es* inhibitors, such as dipyridamole, were significantly more effective as inhibitors of [^{3}H]NBMPR binding and [^{3}H]formycin B uptake by MDCK cells relative to that seen for human cells. We isolated a cDNA encoding the canine *es* nucleoside transporter (designated cENT1), and assessed its function by stable expression in nucleoside transport deficient PK15NTD cells. The PK15-cENT1 cells displayed inhibitor sensitivities that were comparable to those obtained for the endogenous *es* nucleoside transporter in MDCK cells. These data indicate that the dog *es*/ENT1 transporter has distinctive inhibitor binding characteristics, and that these characteristics are a function of the protein structure as opposed to the environment in which it is expressed.

Keywords: Adenosine; Dipyridamole; Draflazine; Nitrobenzylthioinosine; Transporter

1. Introduction

Mammalian cells accumulate nucleosides, such as adenosine, via a variety of transporter proteins that include both Na^+-independent equilibrative and Na^+-dependent concentrative systems (Baldwin et al., 1999). The concentrative transporters (N1/*cif*, N2/*cit*, N3/*cib*) are functionally characterized by their substrate selectivity (Ritzel et al., 2001). The equilibrative transporters, on the other hand, have broadly overlapping substrate specificities and can be functionally subdivided into two distinct systems (*es*, *e*quilibrative *s*ensitive; *ei*, *e*quilibrative *i*nsensitive) based on their sensitivity to the inhibitor nitrobenzylthioinosine (NBMPR) (Hyde et al., 2001). Representatives of both the *es* and *ei* nucleoside transporters, termed ENT1 (equilibrative nucleoside transporter 1) and ENT2 (equilibrative nucleoside transporter 2), respectively, have been cloned from rat, mouse, and human tissues (Yao et al., 1997; Kiss et al., 2000; Griffiths et al., 1997a,b; Handa et al., 2001; Crawford et al., 1998). The *es* nucleoside transporter is generally the most widely expressed and is likely the system responsible for the homeostatic maintenance of biological adenosine levels. Tight regulation of tissue adenosine concentration is expected given the broad neuroprotective, cardioprotective, and vasodilator roles that have been attributed to this endogenous nucleoside (Mubagwa and Flameng, 2001; Tabrizchi and Bedi, 2001; Dunwiddie and Masino, 2001).

The *es* nucleoside transporter is a target for several coronary vasodilator agents, including dipyridamole, dilazep and draflazine. These agents potentiate the endogenous vasodilator activities of adenosine by blocking its re-uptake into cells (Van Belle, 1993, 1995), and it has been proposed that they are also cardioprotective by virtue of their capacities to reduce the loss of interstitial adenosine during ischemia-reperfusion episodes (Deussen, 2000). A complicating factor in the experimental use of these agents is the distinctive species differences in their affinity for the *es* nucleoside transporter (Hammond, 2000; Plagemann and Woffendin, 1988; Williams et al., 1984; Jarvis et al., 1982a). The human transporter is most sensitive to dipyridamole/dilazep/draflazine, followed by mouse and then rat *es*; these differences have been attributed to primary sequence heterogeneity in the N-terminal half of the ENT1 protein

* Corresponding author. Tel.: +1-519-661-3780; fax: +1-519-661-3827.
E-mail address: jhammo@uwo.ca (J.R. Hammond).

0014-2999/$ - see front matter © 2004 Elsevier B.V. All rights reserved.
doi:10.1016/j.ejphar.2004.03.026

(Sundaram et al., 1998). In contrast, numerous studies have shown that the human, mouse and rat *es* nucleoside transporters all have a similar high affinity for the nucleoside analogue NBMPR ($K_D \sim 0.2$ nM), suggesting that the structural determinants of NBMPR binding differ from those of the coronary vasodilators. However, membranes prepared from dog brain (Hammond and Clanachan, 1985), or heart (Williams et al., 1984), have more than a 10-fold lower affinity for [^{3}H]NBMPR than do membranes from other species compared within the same studies. Given that [^{3}H]NBMPR is well established as a high affinity probe for the *es* nucleoside transporter, and its binding affinity has been shown to reflect its potency as a transport inhibitor (Hammond, 2000), these data suggest that the dog *es* nucleoside transporter may be less sensitive to inhibition by NBMPR than that of other species. However, these early studies were based on membrane preparations in which the confirmatory nucleoside flux assays could not be done. Thus, the present study was undertaken to better define the interaction of nucleoside transport inhibitors with the dog *es* nucleoside transporter. As part of this study, we have also cloned the dog ENT1 and generated a stable mammalian cell expression model for functional analysis of the dog ENT1 transporter.

2. Materials and methods

2.1. Materials

MDCK epithelial cells were provided by Dr. L. Dagnino (Physiology and Pharmacology, Univ. of Western Ontario). The PK15-hENT1 and PK15-NTD (*N*ucleoside *T*ransport *D*eficient) cells were provided by Dr. Ming Tse (Johns Hopkins University, USA). PK15-mENT1 cells were created in our laboratory by M. Stolk. [G-^{3}H]Formycin B (14 Ci/mmol) and [G-^{3}H]NBMPR (5.5 Ci/mmol) were purchased from Moravek Biochemicals (Brea, CA, USA), and [^{3}H]water (1 mCi/g) was from DuPont Canada (Markham, Ontario, Canada). Minimum Essential Medium (MEM; with Earle's salts and L-glutamine), fetal bovine serum, and culture grade Dulbecco's phosphate buffered saline were purchased from GIBCO/BRL (Burlington, Ontario, Canada). LipofectAMINE™ 2000 and G418 were obtained from Invitrogen (Burlington, Ontario, Canada). Penicillin G and streptomycin sulphate were purchased from ICN (Montreal, Quebec, Canada). Non-radiolabelled formycin B, NBMPR, nitrobenzylthioguanosine (NBTGR), trypsin-EDTA and dipyridamole (2,6-bis(diethanolamino)-4,8-dipiperidinopyrimido-[5,4-d]pyrimidine) were supplied by Sigma (St. Louis, MO, USA). Dilazep ((*N*,*N*′-bis[3-(3,4,5-trimethoxybenzoyloxy) propyl]-homopiperazine) was provided by Asta Werke (Frankfurt, Germany). Draflazine (2-(aminocarbonyl)-4-amino-2,6-dichlorophenyl)-4-[5,5-bis(4-fluorophenyl)-pentyl]-1-piperazineacetamide 2HCl) and soluflazine (3-(aminocarbonyl)-4-[4,4-(4-fluorophenyl,3-pyridinyl)butyl]-*N*-(2,6-dichlorophenyl)-1-piperazineacetamide 2HCl) were obtained from Janssen Research Foundation (Beerse, Belgium). All compounds used were of reagent grade.

2.2. Cell culture

Cells were cultured in T-175 flasks in MEM plus 10% fetal bovine serum supplemented with penicillin G (100 units/ml) and streptomycin sulphate (100 μg/ml) and maintained in a humidified atmosphere of 5% CO_2 at 37 °C. G418 (500 μg/ml) was included for the PK15-ENT1 stable transfectants to maintain selection pressure. Cells were typically split 1:3 and media was replaced every 3 days. For radioligand binding and/or substrate flux assays, cells were removed from the flasks by trypsinization (0.05%, 10 min, 37 °C), then diluted fourfold with media (+10% fetal bovine serum) and pelleted by centrifugation. The cell pellets were washed once by resuspension/centrifugation in either phosphate buffered saline (PBS; 137 mM NaCl, 6.3 mM Na_2HPO_4, 2.7 mM KCl, 1.5 mM KH_2PO_4, 0.5 mM $MgCl_2{\cdot}6H_2O$, 0.9 mM $CaCl_2{\cdot}H_2O$; pH 7.4), or a modified Na^+-free PBS (iso-osmotic replacement of Na^+ with *N*-methylglucammonium ion, NMG^+) and then resuspended in the same buffer for use in the assays. Cell concentrations were determined using a haemocytometer.

2.3. [^{3}H]NBMPR binding

Cells suspended in PBS ($\sim 2 \times 10^5$/ml) were incubated with [^{3}H]NBMPR (± inhibitors) for 45 min at room temperature ($\sim$ 22 °C) to attain steady-state binding. Solutions were then filtered through Whatman GF/B filters under vacuum, washed twice with Tris–HCl buffer (10 mM, pH 7.4, 4 °C), and analyzed for radioactive content by standard liquid scintillation-counting techniques. Nonspecific binding of [^{3}H]NBMPR was defined as that which remained cell-associated in the presence of NBTGR (10 μM). Specific binding was defined as total minus nonspecific binding. K_D and B_{max} values were calculated from nonlinear (hyperbolic) curve fits (GraphPad Prism 3.02) to non-transformed specific binding data plotted against the free [^{3}H]NBMPR concentration at steady state (see Fig. 1A). Inhibition constants were calculated from variable slope sigmoid curves fitted to the binding of [^{3}H]NBMPR (2 nM), relative to control, against the log of the inhibitor concentration. The Cheng–Prusoff equation (Cheng and Prusoff, 1973) was used to derive K_i values from these studies, using the K_D for [^{3}H]NBMPR obtained by mass law analysis as described above.

2.4. [^{3}H]Formycin B uptake

Unless indicated otherwise, uptake assays were conducted at room temperature in Na^+-free buffer. The use of the Na^+-free buffer ensured that transporter-mediated uptake of [^{3}H]formycin B was due solely to the operation of the

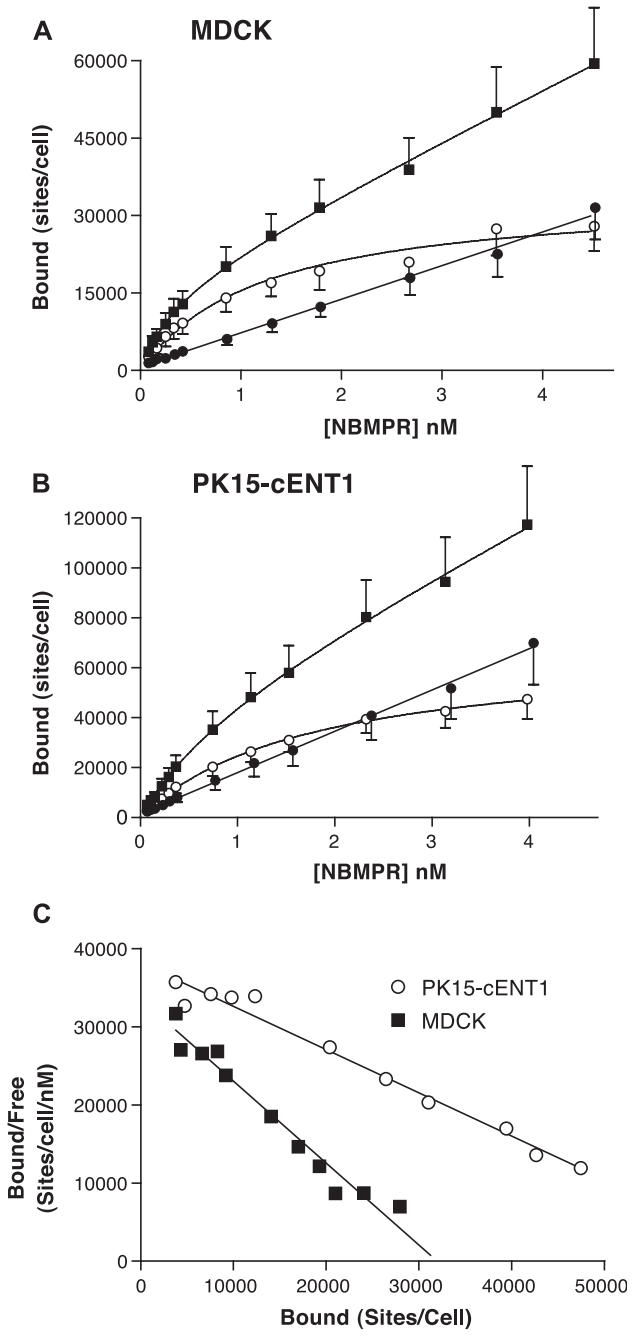

Fig. 1. Mass law analysis of [^{3}H]NBMPR binding. MDCK cells (Panel A) or PK15-cENT1 cells (Panel B) were incubated with a range of concentrations of [^{3}H]NBMPR in the absence (■, total binding) and presence (●, nonspecific binding) of 10 μM NBTGR. Specific binding (○) was defined as the difference between the total and nonspecific binding components. Data are plotted as the number of NBMPR binding sites per cell versus the equilibrium free concentration of [^{3}H]NBMPR. Each point represents the mean ± S.E.M. of five independent experiments. Panel C: Scatchard representations of the specific binding data shown in Panels A and B. Each point is the mean of five experiments. The binding parameters (maximum binding, B_{max}, equilibrium dissociation constant, K_D) derived from these data are shown in Table 1.

Na^+-independent equilibrative transporters (*es* or *ei*) that were the focus of the present study. Uptake was initiated by addition of cell suspension (~ 1×10^6 cells) to [^{3}H]formycin B (10 μM) layered over a 200-μl cushion of silicone oil/mineral oil (21:4 v/v) in 1.5-ml microcentrifuge tubes. Assays were terminated after a defined incubation time by centrifugation of cells through the oil for 10 s at 12,000 × *g*. The supernatant and oil were removed and the cell pellets digested with 1 M sodium hydroxide overnight (~ 16 h) at room temperature. The digest was analyzed for [^{3}H] content by standard liquid scintillation counting techniques. Uptake data are presented as intracellular [^{3}H]substrate concentrations (pmol/μl cell volume; μM) after correction for the amount of [^{3}H]label present in the extracellular space of the cell pellet. Total water volumes of the cell pellets were determined in each experiment by incubating cells with [^{3}H]water for 3 min and then processing the samples as described above. An estimate of the extracellular water volume was obtained from extrapolation of the linear time course of nonmediated uptake to "zero-time". Initial rates (V_i) of flux were estimated as the uptake at 1 s determined by extrapolation of hyperbolic curves fitted (GraphPad Prism 3.02) to time course data, and steady-state intracellular concentrations were estimated by extrapolation of these curves to infinite time. Inhibition constants for selected inhibitors were calculated from variable-slope sigmoid curves fitted to the uptake of 10 μM formycin B, relative to control, against the log of the inhibitor concentration.

2.5. Cloning of the MDCK ENT1 transporter by reverse transcriptase polymerase chain reaction (RT-PCR) and rapid amplification of cDNA ends (RACE)

Polyadenylated RNA (mRNA) was isolated directly from lysed MDCK cells and dog skeletal muscle tissue using the FastTrack 2.0 mRNA Isolation Kit (Invitrogen). First strand cDNA synthesis was performed on 1 μg of mRNA template using the BRL SuperScript™ PreAmplification System (Life Technologies, Burlington, ON) with an oligo(dT)$_{12-18}$ primer. Initial PCR studies were conducted using the Advantage-2 cDNA PCR Polymerase mix from Clontech (Palo Alto, CA) in a Thermocycler PE 480 (Perkin Elmer, Norwalk, CT) using an oil overlaid 50-μl reaction mixture in thin-walled 500-μl tubes. PCR products were resolved by electrophoresis on 1.2% agarose gels, and then gel-purified and ligated directly into pcDNA3.1/V5-His TOPO vector (pcDNA3.1) and propagated in One Shot TOP10 Chemically Competent *E. coli* using protocols provided by the supplier (Invitrogen). The plasmid inserts were sequenced in both directions by *Taq* BigDye Terminator Cycle Sequencing Kit using an automated ABI PRISM Model 377 Version 3.3 DNA Sequencer (PE Applied Biosystems, Norwalk, CT).

A section of the coding region of the MDCK c(canine)ENT1 was obtained initially by RT-PCR using primers designed against highly conserved regions of the human,

Table 1
[^{3}H]NBMPR binding and [^{3}H]formycin B uptake by a series of PK15-cENT1 clonal cell lines

Cell line	[^{3}H]NBMPR binding		[^{3}H]Formycin B uptake
	B_{max} (sites/cell)	K_D (nM)	V_i (pmol/μl/s)
MDCK	32,000 ± 4000	1.3 ± 0.3	0.055 ± 0.008
PK15-cENT1-5	22,000 ± 3000	1.4 ± 0.2	0.018 ± 0.007
PK15-cENT1-6	64,000 ± 18,000	2.1 ± 0.6	nd
PK15-cENT1-12	46,000 ± 3000	1.8 ± 0.2	0.051 ± 0.014
PK15-cENT1-14	75,000 ± 13,000	2.2 ± 0.6	0.034 ± 0.006
PK15-cENT1-15	128,000 ± 17,000	4.0 ± 0.7	0.133 ± 0.013
PK15-cENT1-18	71,000 ± 10,000	1.8 ± 0.2	nd
PK15-hENT1	39,000 ± 7000	0.10 ± 0.01	nd
PK15-mENT1	55,000 ± 16,000	0.30 ± 0.08	0.23 ± 0.07

Binding B_{max} and K_D values for [^{3}H]NBMPR were derived from hyperbolic curves fitted to data such as that shown in Fig. 1. The initial rates (V_i) of transporter-mediated [^{3}H]formycin B (10 μM) influx were estimated from hyperbolic curves fitted to data points calculated as the difference between the total uptake and the non-mediated uptake (see Fig. 3). Data obtained in parallel studies for [^{3}H]NBMPR binding to PK15 cells transfected with the human (PK15-hENT1) or mouse (PK15-mENT1) ENT1 transporter are included for comparison (Stolk and Hammond, unpublished). Each value is the mean ± S.E.M. from at least five independent experiments conducted in duplicate. nd = not determined.

mouse and rat ENT1 (Genbank accessions #U81375, #AF305501, and AF015304, respectively). The sense primer corresponded to bases 410–434 of hENT1 (5′-GCCATCTTCAACAATGTCATGACCC-3′) and the antisense primer corresponded to bases 1402–1425 of hENT1 (5′-CACATGCAGAGGCTGGCGAGGTAG-3′). Amplification parameters were: (A) 94 °C for 3 min; (B) 94 °C for 1 min, 61 °C for 1 min, 72 °C for 1 min (35 cycles); (C) 72 °C for 10 min. The remaining 3′ sequence, including the untranslated region, was obtained by 3′-Rapid Amplification of cDNA Ends (3′RACE) using the Marathon cDNA Amplification Kit (Clontech). The gene-specific primer, designed from the partial cENT1 sequence obtained above, was 5′-CCTGGGCAGCCTGATAGCCATCC-3′ (corresponding to nt 514–536 of hENT1). The complementary primer was the AP1 oligonucleotide provided by Clontech, designed to hybridize with the Clontech RACE Adaptor. PCR parameters were based on manufacturer's recommendations for touch-down, two-step PCR. The first set of parameters were: (A) 5 cycles at 94 °C for 30 s, 72 °C for 4 min; (B) 5 cycles at 94 °C for 30 s, 70 °C for 4 min; (C) 30 cycles at 94 °C for 20 s, 66 °C for 4 min. The secondary PCR used the AP2 primer (Clontech) and a nested GSP (5′-GCCTGATAGCCATCCTGTTGGTGTTCC-3′; corresponding to nt 522–548 of hENT1), designed from the partial cENT1 sequence described above, with similar parameters except that the number of cycles was reduced to 20 in step C. Similar attempts to obtain the remaining 5′ sequence by 5′-RACE were unsuccessful. Therefore, a sense primer was designed to the 5′-untranslated region of the hENT1 sequence, just upstream from the start codon, that was conserved in the ENT1 of human, mouse, and rat (5′-TCAGCCAGGGAAAACCGAGAACAC-3′), and paired with an antisense primer (5′-GGATTCCTCTTTGTTTGCCACTGGC-3′; corresponding to nt 952–976 of hENT1) based on the partial cENT1 sequence confirmed above. RT-PCR was then performed using the following cycling parameters: (A) 95 °C for 1 min, (B) 30 cycles of 95 °C for 30 s, 62 °C for 2 min, (C) 62 °C for 3 min, followed by extension at 70 °C for 10 min. The PCR products obtained in this reaction were then used as the template for a second round of PCR with the same sense primer and a nested antisense primer (5′-GGTAGAACTCCAGTCGGGGCAGGA-3′ (corresponding to nt 852–875 of hENT1). The PCR cycling parameters were the same as for the primary PCR reaction but with 20 cycles in step B.

The cDNA corresponding to the complete open reading frame of MDCK cENT1 was then obtained by RT-PCR using the proof-reading polymerase *Pfx* (Platinum *Pfx*; Invitrogen), a sense primer flanking the translation start codon, and an antisense primer to the 3′ end of the coding region. Both primers had *Kpn*I restriction sites engineered at the 5′ ends to facilitate future construct generation (sense: 5′-CGGGGTACCGCCACCATGACAACCAGTC-3′; antisense: 5′-GCCGGGTACCAAGGCACCTGGTTTCTGT-

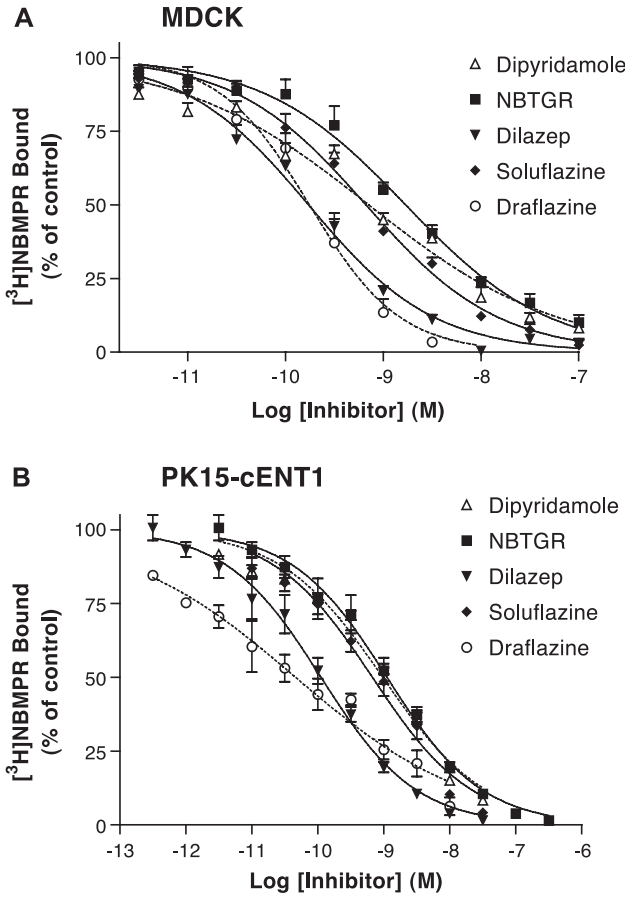

Fig. 2. Inhibition of [^{3}H]NBMPR binding to MDCK (Panel A) and PK15-cENT1 (Panel B) cells. Data are shown as percent of control binding where the "control" was the site-specific binding of 2.0 nM [^{3}H]NBMPR in the absence of inhibitor. Each point represents the mean ± S.E.M. from five experiments conducted in duplicate. K_i values derived from these data are shown in Table 2.

3′). The resulting 1400-bp band was ligated directly into pcDNA3.1 and sequenced in both directions to confirm integrity. To ensure that the ENT1 cDNA isolated from MDCK cells was representative of the dog ENT1 transporter, the corresponding cDNA was amplified by RT-PCR (using Pfx polymerase) from dog skeletal muscle tissue and sequenced as described above.

Amino acid sequences were deduced from the nucleotide open reading frame and the potential membrane-spanning regions and orientation were determined with the TMpred program (http://www.ch.embnet.org/software/TMPRED_form.html). Consensus sequences for potential post-translational processing sites were identified using Prosite (http://www.expasy.ch/prosite/). MACAW (Multiple Alignment Construction and Analysis Workbench, NCBI, version 2.0.5) was used to align the translated amino acid sequence of cENT1 with the rat, mouse, and human ENT1 sequences (see Fig. 5). ISIS Draw 2.4 (MDL Information Systems, San Leandro, CA) was used to construct the topology representation shown in Fig. 6.

2.6. Stable transfection of PK15-NTD cells

The pcDNA3.1-cENT1 coding region construct, obtained as described above, was transfected into the PK15-NTD cell line using LipofectAMINE™ 2000 based on protocols supplied by the manufacturer (Invitrogen). Briefly, plasmid DNA (5 μg per well for a six-well plate) was linearized with *Pvu*I and diluted to 250 μl with MEM (without serum or antibiotics) and added to 250 μl of a 1:50 dilution (in serum/antibiotic free MEM) of LipofectAMINE™ 2000. Following a 6-h incubation at 37 °C, fetal bovine serum was added to bring the serum concentration to 5%. G418 (500 μg/ml) was added to the culture starting 48 h post-transfection, and maintained for 2 weeks, to eliminate cells not expressing the resistance gene associated with the pcDNA3.1 vector. This concentration of G418 was found, in preliminary studies, to be sufficient to kill over 99% of the non-transfected PK15-NTD cells. The transfected cells remaining after 2 weeks of G418 treatment (typically <10%) were diluted onto a series of 10-cm^2 plates such that individual cell colonies could be discerned. Once colonies reached a size of approximately 300 cells, they were isolated using cloning cylinders and transferred to 24-well plates. Cells, maintained in 500μg/ml G418, were then sequentially passaged up to T-175 flasks to obtain sufficient cells for assay of ENT activity.

3. Results

3.1. [^{3}H]NBMPR binding by MDCK cells

The total binding profile of the *es*-specific radioligand [^{3}H]NBMPR fit best to a two-component model with the low affinity component equivalent to that seen in the presence of NBTGR (nonspecific binding). Subtraction of the nonspecific binding component, which was linear with [^{3}H]NBMPR concentration, from the total binding resulted in a saturable binding profile representing 32,800 ± 5200 [^{3}H]NBMPR binding sites per cell with a K_D of 1.3 ± 0.3 nM (Fig. 1A, Table 1). Scatchard analyses of these data yielded a linear plot, confirming a single class of specific [^{3}H]NBMPR binding sites, with a Hill coefficient of 1.00 ± 0.01 (Fig. 1B). Assuming that one molecule of NBMPR binds to one *es* nucleoside transporter (Jarvis et al., 1982b), this means the MDCK cells have ~ 32,800 *es* nucleoside transporters per cell. A series of known inhibitors of nucleoside transport were then tested for their ability to inhibit the binding of [^{3}H]NBMPR (2 nM) to MDCK cells. All of the agents tested inhibited binding in a monophasic manner (Fig. 2A). Draflazine and dilazep were the most potent with K_i values of less than 0.012 nM, followed by soluflazine and dipyridamole (Table 2). The least effective of the high-affinity inhibitors tested was NBTGR with a K_i of 0.74 ± 0.10 nM. Formycin B, a substrate for the *es* nucleoside transporter, had a K_i of 139 ± 35 μM (data not shown).

Table 2
Inhibition of [^{3}H]NBMPR binding and [^{3}H]formycin B uptake by established inhibitors of the *es* nucleoside transporter

Inhibitor	[^{3}H]NBMPR binding (K_i, nM)				[^{3}H]Formycin B uptake (K_i, nM)		
	Dog MDCK	PK15-cENT1	Human erythrocytes	Mouse Ehrlich cells	Dog MDCK	PK15-cENT1	PK15-hENT1
NBMPR	1.3 ± 0.3[a,b]	2.2 ± 0.2[a,b]	0.15 ± 0.04[a]	0.11 ± 0.02[a]	2.7 ± 0.6[b]	2.1 ± 0.9[b]	0.5 ± 0.2
NBTGR	0.74 ± 0.10[b]	0.72 ± 0.20[b]	0.23 ± 0.05	0.18 ± 0.02			
Dipyridamole	0.27 ± 0.03[b]	0.52 ± 0.03[b]	1.9 ± 0.4	77 ± 2	0.43 ± 0.07[b]	1.4 ± 0.5[b]	11 ± 5
Soluflazine	0.26 ± 0.03[b]	0.38 ± 0.07[b]	1.8 ± 0.2	780 ± 54	–	–	–
Draflazine	0.11 ± 0.02[b]	0.03 ± 0.01[b]	0.28 ± 0.03	10 ± 3	0.38 ± 0.09	–	–
Dilazep	0.08 ± 0.02[b]	0.09 ± 0.01[b]	0.29 ± 0.05	2.7 ± 0.1	0.43 ± 0.09	–	–

K_i values were calculated from IC_{50} values derived from curves such as those shown in Figs. 2 and 4 using the Cheng–Prusoff equation (Cheng and Prusoff, 1973). For the inhibition of formycin B uptake analyses, the K_i (139 μM) for formycin B inhibition of [^{3}H]NBMPR binding to MDCK cells was used as an estimate of the K_m of formycin B for the dog *es*/ENT1 transporter. Data obtained by our laboratory (using identical methodology) for inhibition of [^{3}H]NBMPR binding to human erythrocytes and mouse Ehrlich cells (Hammond, 1991, 2000) are shown for comparison. Each value is the mean ± S.E.M. from at least five independent experiments conducted in duplicate.

[a] K_D values for site-specific binding of [^{3}H]NBMPR.

[b] Significantly different from the corresponding value obtained in the human cell model (two-tailed Students t-test, $P<0.05$).

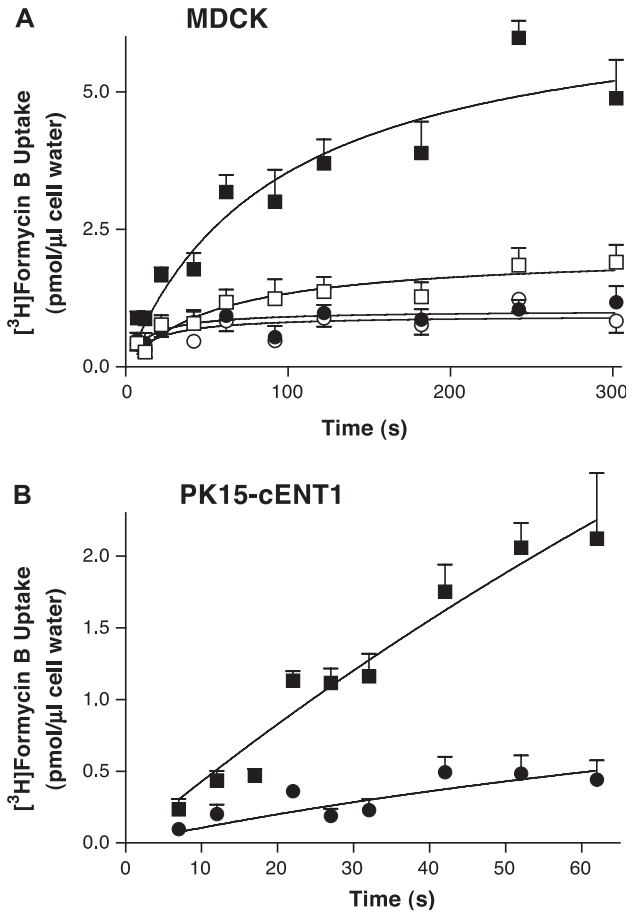

Fig. 3. Time course of [^{3}H]formycin B accumulation by MDCK cells and PK15-cENT1 transfectants. Panel A: MDCK cells were incubated with 10 µM [^{3}H]formycin B in the absence (■, "Total" uptake) and presence of 50 nM NBMPR (□, "NBMPR-resistant" uptake) or 10 µM dipyridamole/NBMPR (to inhibit all equilibrative transporter activity; ●, "Non-mediated"), or 10 µM dipyridamole/10 µM NBMPR/10 mM adenosine (○) for the times indicated (abscissa). Panel B: PK15-cENT1 cells were incubated with 10 µM [^{3}H]formycin B in the absence (■, "Total" uptake) and presence of 10 µM dipyridamole/NBMPR (●, "Nonmediated") for the times indicated (abscissa). Note the shorter time profile used in Panel B. All uptake assays were conducted in Na^+-free buffer and terminated by the oil-stop method described in the text. Initial rates of transporter-mediated uptake, derived from these experiments, are shown in Table 1. Each point represents the mean ± S.E.M. from five experiments.

3.2. [^{3}H]Formycin B uptake by MDCK cells

MDCK cells accumulated [^{3}H]formycin B (10 µM) to a maximum of 6.8 ± 1.0 pmol/µl of cell water. The rate of uptake in the presence of 150 nM NBMPR was reduced significantly, and uptake was blocked almost completely by a combination of 10 µM NBMPR and 10 µM dipyridamole (Fig. 3A). No significant difference in [^{3}H]formycin B uptake was observed when assays were conducted in the presence or absence of Na^+ (data not shown), and the addition of adenosine to assays already containing dipyridamole and NBMPR had no further inhibitory effect on the cell accumulation of [^{3}H]formycin B (Fig. 3A). This shows that MDCK cells do not express a concentrative nucleoside transporter with affinity for formycin B; hence, cell-associated [^{3}H]formycin B in the presence of NBMPR/dipyridamole was considered to be transporter-independent (non-mediated). Total transporter-mediated uptake (total minus nonmediated) occurred with an initial rate (V_i) of 0.055 ± 0.008 pmol/µl/s. Uptake of formycin B by the *ei*-like transporter (NBMPR-resistant uptake minus non-mediated uptake) represented only 13 ± 5% of the total transporter-mediated uptake with a V_i of 0.007 ± 0.003 pmol/µl/s; the remaining 0.048 pmol/µl/s that was NBMPR-sensitive was likely due to the activity of the *es* transport system. Dipyridamole, dilazep, and draflazine inhibited the total mediated uptake of [^{3}H]formycin B in a concentration-dependent manner (Fig. 4A) with IC_{50} values not significantly different from each other (~ 0.5 nM). NBMPR, on the other hand, was significantly less effective with an IC_{50} of 2.9 ± 0.6 nM (Fig. 4A). K_i estimates derived from these IC_{50} values are shown in Table 2.

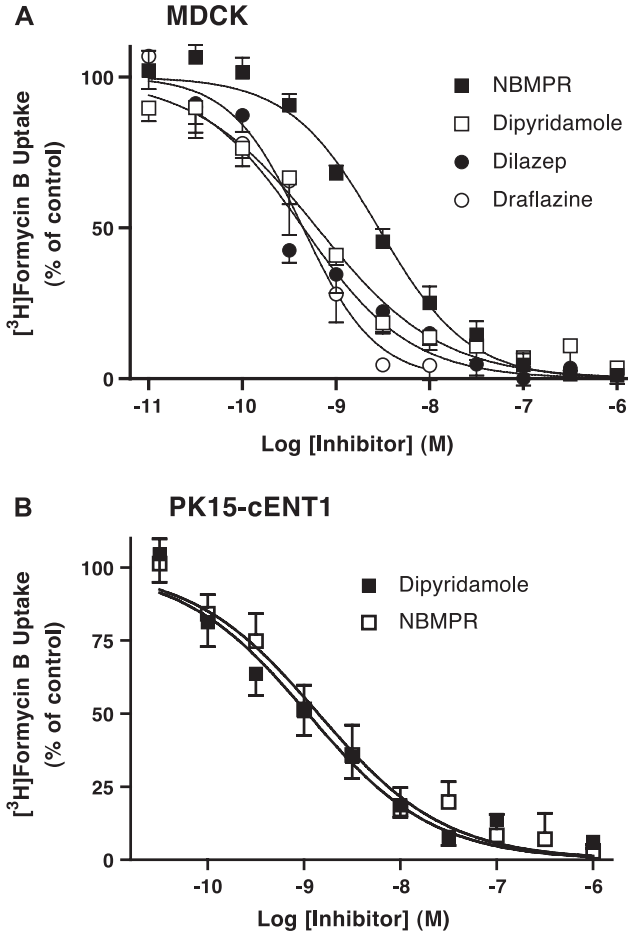

Fig. 4. Inhibition of transporter-mediated [^{3}H]formycin B uptake. MDCK cells (Panel A) or PK15-cENT1 cells (Panel B) were incubated with 10 µM [^{3}H]formycin B for 15 s in the presence or absence of the indicated concentrations of inhibitors. Data are shown as percent of control uptake where the "control" was the transporter-mediated uptake of formycin B in the absence of inhibitor. Each point represents the mean ± S.E.M. from five experiments conducted in duplicate. K_i values derived from these data are shown in Table 2.

3.3. RT-PCR

The oligonucleotide sequence corresponding to the MDCK ENT1 transporter had an open reading frame of 1368 bases and a 611-base 3′-UTR. The corresponding ENT1 cDNA derived by RT-PCR from dog skeletal muscle mRNA was identical with the exception of one synonymous base change (C/T) at position 70 of the MDCK ENT1 sequence. The encoded protein consisted of 456 amino acids with 92/87%, 85/76%, and 85/74% similarity/identity with the human, mouse and rat ENT1 polypeptide, respectively. The complete sequence alignments are shown in Fig. 5. Hydropathy analysis predicted 11 transmembrane domains, similar to that predicted for the human, mouse and rat ENT1 transporters (Griffiths et al., 1997a; Yao et al., 1997; Kiss et al., 2000). The TMpred (http://www.ch.embnet.org/software/TMPRED_form.html) analysis also predicted an extracellular N-terminus. However, it has been established using peptide specific antibodies that hENT1 has an intracellular N-terminus orientation (Sundaram et al., 2001a) and it is expected that the canine (c)ENT1 would have a similar orientation (Fig. 6).

3.4. Characterization of PK15-cENT1 stable transfectants

Twenty independent cell colonies were selected from culture plates after limiting dilution of the PK15 cells transfected with pcDNA3.1-cENT1. Each cell line was screened for specific [^{3}H]NBMPR binding activity using a three-point assay (0.2, 0.8, and 2 nM), and six of these cell lines were chosen for more extensive examination of [^{3}H]NBMPR binding and [^{3}H]formycin B uptake. Mass law analysis of the binding of 12 concentrations of [^{3}H]NBMPR to these cell lines resulted in a range of binding site densities from 22,000 sites/cell to 128,000 sites/cell with an average K_D of 2.2 nM (Fig. 1B and C,

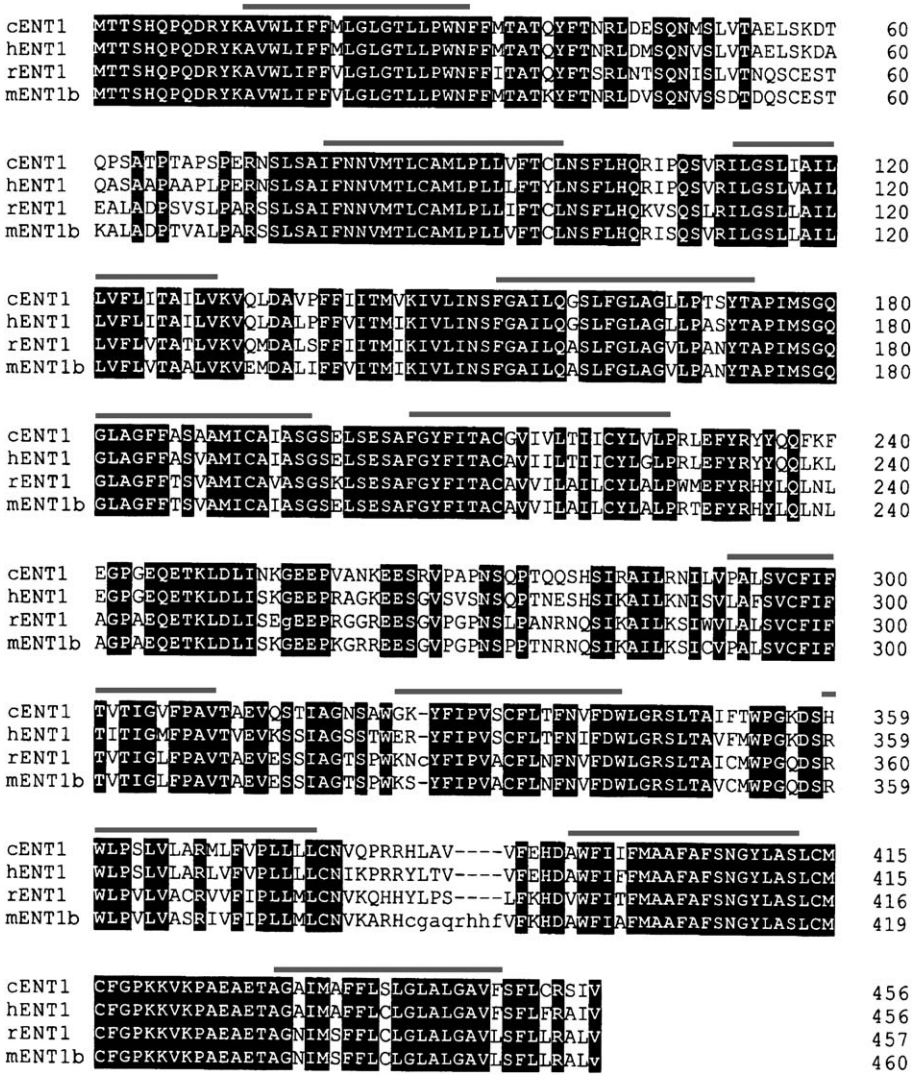

Fig. 5. Alignment of the predicted amino acid sequences of cENT1 with hENT1, rENT1 and mENT1b. Amino acid sequences were deduced from the nucleotide open reading frames for each cDNA. Shaded backgrounds represent residues that are conserved across all four species. The bars above each row represent the predicted transmembrane regions of cENT1.

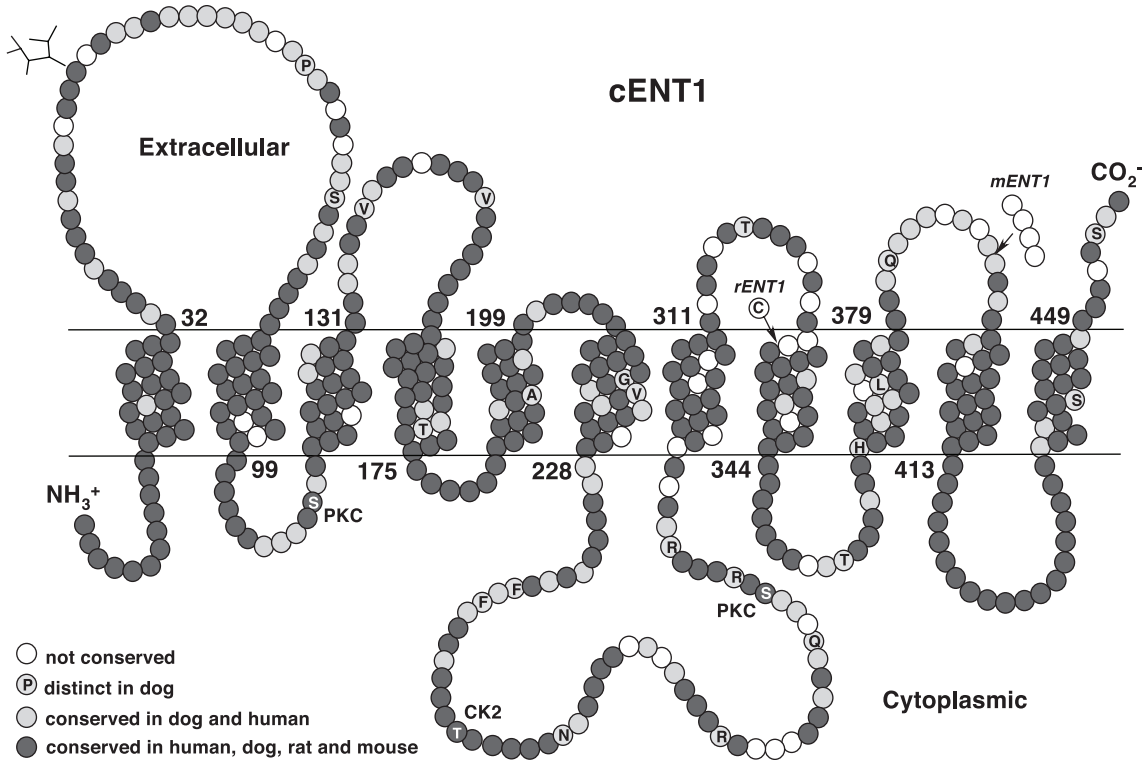

Fig. 6. Topological model of cENT1—comparison with rodent (rat, mouse) and human orthologues. Potential membrane-spanning regions were determined with the TMpred program. Potential N-linked glycosylation sites are indicated by "branching lines", and putative serine/threonine phosphorylation sites are indicated by the associated protein kinase (PKC, protein kinase C; CK2, casein kinase 2). Residues conserved across all four species are shown as dark grey circles; residues that are identical in human and canine ENT1 but differ from those in the rodent orthologues are shown as empty light grey circles. Residues that are distinct in cENT1, but conserved in the other three species, are shown in light grey circles containing the single letter code for the amino acid in cENT1. Open (unfilled) circles represent those residues which are not conserved between species and do not fall into one of the categories described above.

Table 1). [^{3}H]NBMPR binding (2 nM) to the PK15-cENT1 cells was inhibited by a series of compounds with an order of potency (draflazine>dilazep>soluflazine>dipyridamole>NBTGR) similar to that seen for MDCK cells (Fig. 2B, Table 2). The rate of uptake of 10 μM [^{3}H]formycin B by the PK15-cENT1 cell lines (Fig. 3B) generally parallelled their [^{3}H]NBMPR binding site densities with initial rates (V_i) ranging from 0.017 to 0.133 pmol/μl/s (Table 1). Dipyridamole and NBMPR inhibited the uptake of [^{3}H]formycin B in a consistent manner across all PK15-cENT1 cell lines (pooled data shown in Fig. 4B) with K_i values of 2.1 ± 0.9 nM for NBMPR and 1.4 ± 0.5 nM for dipyridamole (Table 2). The aforementioned K_i values as well as the [^{3}H]NBMPR binding K_D values obtained for the PK15-cENT1 cells were significantly different from those derived using equivalent experimental procedures from PK15 cells stably transfected with either the human (Ward et al., 2000) or mouse (Stolk and Hammond, unpublished) ENT1 transporter (Tables 1 and 2).

4. Discussion

Nucleoside transporters play important roles in the regulation of extracellular adenosine concentrations and, ergo, the biological activity of adenosine at its specific extracellular receptors. One of the most studied aspects of adenosine biology is its role as a vasodilator and cardioprotectant (Mubagwa and Flameng, 2001; Tabrizchi and Bedi, 2001). It has been shown that enhancement of adenosine levels by blockade of its uptake and metabolism can enhance the beneficial cardiovascular effects of adenosine (Van Belle, 1993, 1995). Nucleoside transport inhibitors have also been studied for their ability to improve the survival of donor hearts for transplantation (Flameng et al., 1991; Yang et al., 1994). Many of these studies have been done using dog models of cardiac function. Early studies on the binding of [^{3}H]NBMPR to nucleoside transporters suggested that dog membranes had a lower affinity for this *es*-selective nucleoside transport inhibitor than did membranes from other species (Williams et al., 1984; Hammond and Clanachan, 1985). However, since these studies were done in isolated membranes, the confirmatory nucleoside flux studies could not be done.

Using MDCK cells, as well as PK15 cells transfected with recombinant cENT1, we have shown that the relatively low affinity [^{3}H]NBMPR binding sites do correspond to *es*/ENT1 transporters that are less sensitive to inhibition by NBMPR than that seen in other species. This conclusion was made based predominantly on comparative studies done

in our laboratory using cells from different species (Hammond, 1991, 2000; Vyas et al., 2002), where the critical methodological variables in the binding assay (cell preparation, buffer composition, temperature, filtration procedure, equilibration time) were consistently controlled. We have also shown that MDCK cells express an ENT1 transporter that is identical in primary sequence to that isolated from dog skeletal muscle, confirming the validity of the MDCK cells as a canine nucleoside transport model. MDCK cells bound [^{3}H]NBMPR with a K_D of 1.3 nM, which is almost 10-fold lower than the K_D for this radioligand in cell lines from other species (see Table 2), but is similar to that determined in previous studies using membranes from dog heart (Williams et al., 1984) and brain (Hammond and Clanachan, 1985). NBMPR also inhibited [^{3}H]formycin B uptake by MDCK and PK15-hENT1 cells with a potency (K_i = 2.7 nM) that was consistent with its lower binding affinity. A related compound, NBTGR, was also found to inhibit [^{3}H]NBMPR binding to the canine transporter (both MDCK and PK15-cENT1 cells) with an affinity that was significantly lower than that seen for mouse and human cell models. This reduction in inhibitor potency was restricted to the nucleoside derivatives NBMPR and NBTGR, since other ENT1 inhibitors such as dipyridamole, dilazep, and draflazine were actually more effective at inhibiting [^{3}H]NBMPR binding in the dog cell models compared to that seen in human erythrocytes (Table 2). It is noteworthy that all of the compounds tested had relatively shallow slopes for inhibition of [^{3}H]NBMPR binding to the PK15-cENT1 cells, when compared with MDCK cells (see Fig. 2). Similar complex inhibition profiles (shallow or biphasic curves) have been noted for the same PK15 cells transfected with the human (Hammond and Archer, 2004) or mouse (Stolk and Hammond, unpublished) ENT1 transporters, and may reflect anomalous post-translational processing of a subset of the recombinant ENT1 transporters expressed by these cells.

MDCK cells express predominantly the *es* subtype of equilibrative nucleoside transporter, although a measurable (13%) component of the *ei* subtype was also present. The relative roles of the *es* and *ei* nucleoside transporters in the regulation of cell nucleoside metabolism are currently unknown, although it has been shown that the human *ei* nucleoside transporter, unlike *es*, can accept nucleobases as substrates in addition to purine and pyrimidine nucleosides (Yao et al., 2002). We found no evidence for the operation of a Na^+-dependent concentrative transporter for formycin B in MDCK cells, consistent with previous reports (Mangravite et al., 2001).

Nucleoside transporters have been implicated in the cellular uptake of cytotoxic nucleosides used in antiviral and anticancer therapy (Belt et al., 1993; Mackey et al., 1998), and are the primary targets for a number of established and potential cardioprotective and neuroprotective agents. Therefore, it is important to understand how inhibitors and substrates interact with these transport proteins. Delineation of the structure–function relationships for existing ligands may facilitate the development of more efficacious and selective nucleoside transport inhibitors. Considerable attention has been paid recently to the sites of interaction for the vasodilators dipyridamole and dilazep (Visser et al., 2002; Vickers et al., 1999; Sundaram et al., 1998). Using the well-known species differences in sensitivity of the *es* nucleoside transporter to dipyridamole and dilazep (rat < mouse < human), chimeric transporters were used to establish that these inhibitors interact with a site that is distinct from, but likely overlaps with, the NBMPR binding site (Sundaram et al., 1998). The attainment of the canine ENT1 (cENT1) sequence will now allow development of chimeric proteins and site-directed mutants to define the critical differences in the dog transporter that result in the lower NBMPR affinity (Figs. 5 and 6).

ENT1 sequence alignments shown in Fig. 5, and displayed schematically in Fig. 6, highlight a number of regions with significant differences in amino acid properties between the dog ENT1 and that of other species. As might be anticipated, there was a strong similarity with the hENT1 transporter sequence. The light grey circles in Fig. 6 represent those residues that are conserved in human and dog (high affinity for dilazep/dipyridamole/draflazine) but differ from rat and mouse (lower affinity for dilazep/dipyridamole/draflazine). cENT1 shares the methionine at position 33 with hENT1—this methionine appears to be important for the high affinity binding of dipyridamole and dilazep (Visser et al., 2002). A conserved glycine in transmembrane domain 5 (G179) of hENT1 has been shown to be critical for transport function and NBMPR binding (SenGupta et al., 2002). This glycine is in the middle of a conserved stretch of 15 amino acids (172–186) that is flanked by two residues with distinctly different properties in cENT1 (T170, A189) compared to the other species (A170, V189). Transmembrane regions 3 and 4 (plus the adjoining extracellular loop) have also been implicated in the binding of NBMPR (Sundaram et al., 2001b). In this regard, there are two valines (V137, V145) in the second extracellular loop of cENT1 that are either leucines (L137) or isoleucines (I145) in all of the other species. It is possible that any or all of these structural differences contribute to a conformation of the protein with reduced affinity for NBMPR yet enhanced affinity for coronary vasodilators such as dilazep. These data provide rational starting points for the design of site-directed ENT1 mutants for future structure–function studies.

In summary, our data show that the relatively low affinity binding sites for [^{3}H]NBMPR in dog membranes do represent *es*/ENT1 transporters that are relatively less sensitive to inhibition by NBMPR than are the human, mouse, and rat *es* nucleoside transporters. This atypical sensitivity to widely used nucleoside transport inhibitors needs to be considered when these agents are employed in dog experimental models to assess the actions of purinergic receptor drugs and nucleoside metabolic modifiers. This is the first report

of a cDNA corresponding to the canine NBMPR-sensitive equilibrative nucleoside transporter (cENT1). The availability of this cDNA will assist further studies aimed at the delineation of protein domains involved in the interaction of inhibitors with the ENT1 transporter. The development of the PK15-cENT1 expression model, along with parallel cell models expressing the human (Ward et al., 2000) or mouse (Stolk and Hammond, unpublished) ENT1 transporters, will also provide a unique screening system for new inhibitors and substrates of nucleoside transporters.

Acknowledgements

This study was supported by a grant to J.R.H. from the Canadian Institutes of Health Research. During the course of this work, M.S. was supported by an Ontario Graduate Scholarship and a Postgraduate Scholarship from the Natural Sciences and Engineering Research Council of Canada. The expert technical assistance of Václav Pitelka is also gratefully acknowledged.

References

Baldwin, S.A., Mackey, J.R., Cass, C.E., Young, J.D., 1999. Nucleoside transporters: molecular biology and implications for therapeutic development. Mol. Med. Today 5, 216–224.

Belt, J.A., Marina, N.M., Phelps, D.A., Crawford, C.R., 1993. Nucleoside transport in normal and neoplastic cells. Adv. Enzyme Regul. 33, 235–252.

Cheng, Y., Prusoff, W.H., 1973. Relationship between the inhibition constant (K1) and the concentration of inhibitor which causes 50 per cent inhibition (I50) of an enzymatic reaction. Biochem. Pharmacol. 22, 3099–3108.

Crawford, C.R., Patel, D.H., Naeve, C., Belt, J.A., 1998. Cloning of the human equilibrative, nitrobenzylmercaptopurine riboside (NBMPR)-insensitive nucleoside transporter *ei* by functional expression in a transport-deficient cell line. J. Biol. Chem. 273, 5288–5293.

Deussen, A., 2000. Metabolic flux rates of adenosine in the heart. Naunyn-Schmiedeberg's Arch. Pharmacol. 362, 351–363.

Dunwiddie, T.V., Masino, S.A., 2001. The role and regulation of adenosine in the central nervous system. Annu. Rev. Neurosci. 24, 31–55.

Flameng, W., Sukehiro, S., Mollhoff, T., Van Belle, H., Janssen, P., 1991. A new concept of long-term donor heart preservation: nucleoside transport inhibition. J. Heart Lung Transplant. 10, 990–998.

Griffiths, M., Beaumont, N., Yao, S.Y.M., Sundaram, M., Boumah, C.E., Davies, A., Kwong, F.Y.P., Coe, I., Cass, C.E., Young, J.D., Baldwin, S.A., 1997a. Cloning of a human nucleoside transporter implicated in the cellular uptake of adenosine and chemotherapeutic drugs. Nat. Med. 3, 89–93.

Griffiths, M., Yao, S.Y., Abidi, F., Phillips, S.E., Cass, C.E., Young, J.D., Baldwin, S.A., 1997b. Molecular cloning and characterization of a nitrobenzylthioinosine-insensitive (ei) equilibrative nucleoside transporter from human placenta. Biochem. J. 328, 739–743.

Hammond, J.R., 1991. Kinetic analysis of ligand binding to the Ehrlich cell nucleoside transporter: pharmacological characterization of allosteric interactions with the [^{3}H]nitrobenzylthioinosine binding site. Mol. Pharmacol. 39, 771–779.

Hammond, J.R., 2000. Interaction of a series of draflazine analogues with equilibrative nucleoside transporters: species differences and transporter subtype selectivity. Naunyn-Schmiedeberg's Arch. Pharmacol. 361, 373–382.

Hammond, J.R., Archer, R.G., 2004. Interaction of the novel adenosine uptake inhibitor 3-[1-(6,7-diethoxy-2-morpholinoquinazolin-4-yl)piperidin-4-yl]-1,6-dimethyl-2,4(1*H*,3*H*)-quinazolinedione hydrochloride (KF24345) with the *es* and *ei* subtypes of equilibrative nucleoside transporters. J. Pharmacol. Exp. Ther. 308, 1083–1093.

Hammond, J.R., Clanachan, A.S., 1985. Species differences in the binding of [^{3}H]nitrobenzylthioinosine to the nucleoside transport system in mammalian central nervous system membranes: evidence for interconvertible conformations of the binding site/transporter complex. J. Neurochem. 45, 527–535.

Handa, M., Choi, D., Caldeiro, R.M., Messing, R.O., Gordon, A.S., Diamond, I., 2001. Cloning of a novel isoform of the mouse NBMPR-sensitive equilibrative nucleoside transporter (ENT1) lacking a putative phosphorylation site. Gene 262, 301–307.

Hyde, R.J., Cass, C.E., Young, J.D., Baldwin, S.A., 2001. The ENT family of eukaryote nucleoside and nucleobase transporters: recent advances in the investigation of structure/function relationships and the identification of novel isoforms. Mol. Membr. Biol. 18, 53–63.

Jarvis, S.M., Hammond, J.R., Paterson, A.R.P., Clanachan, A.S., 1982a. Species differences in nucleoside transport. Biochem. J. 208, 83–88.

Jarvis, S.M., McBride, D., Young, J.D., 1982b. Erythrocyte nucleoside transport: asymmetrical binding of nitrobenzylthioinosine to nucleoside permeation sites. J. Physiol. (Lond.) 324, 31–46.

Kiss, A., Farah, K., Kim, J., Garriock, R.J., Drysdale, T.A., Hammond, J.R., 2000. Molecular cloning and functional characterization of inhibitor-sensitive (mENT1) and inhibitor-resistant (mENT2) equilibrative nucleoside transporters from mouse brain. Biochem. J. 352 (Pt. 2), 363–372.

Mackey, J.R., Baldwin, S.A., Young, J.D., Cass, C.E., 1998. Nucleoside transport and its significance for anticancer drug resistance. Drug Resist. Updat. 1, 310–324.

Mangravite, L.M., Lipschutz, J.H., Mostov, K.E., Giacomini, K.M., 2001. Localization of GFP-tagged concentrative nucleoside transporters in a renal polarized epithelial cell line. Am. J. Physiol., Renal Physiol. 280, F879–F885.

Mubagwa, K., Flameng, W., 2001. Adenosine, adenosine receptors and myocardial protection: an updated overview. Cardiovasc. Res. 52, 25–39.

Plagemann, P.G.W., Woffendin, C., 1988. Species differences in sensitivity of nucleoside transport in erythrocytes and cultured cells to inhibition by nitrobenzylthioinosine, dipyridamole, dilazep, and lidoflazine. Biochim. Biophys. Acta 969, 1–8.

Ritzel, M.W., Ng, A.M., Yao, S.Y., Graham, K., Loewen, S.K., Smith, K.M., Hyde, R.J., Karpinski, E., Cass, C.E., Baldwin, S.A., Young, J.D., 2001. Recent molecular advances in studies of the concentrative Na+-dependent nucleoside transporter (CNT) family: identification and characterization of novel human and mouse proteins (hCNT3 and mCNT3) broadly selective for purine and pyrimidine nucleosides (system cib). Mol. Membr. Biol. 18, 65–72.

SenGupta, D.J., Lum, P.Y., Lai, Y., Shubochkina, E., Bakken, A.H., Schneider, G., Unadkat, J.D., 2002. A single glycine mutation in the equilibrative nucleoside transporter gene, hENT1, alters nucleoside transport activity and sensitivity to nitrobenzylthioinosine. Biochemistry 41, 1512–1519.

Sundaram, M., Yao, S.Y., Ng, A.M., Griffiths, M., Cass, C.E., Baldwin, S.A., Young, J.D., 1998. Chimeric constructs between human and rat equilibrative nucleoside transporters (hENT1 and rENT1) reveal hENT1 structural domains interacting with coronary vasoactive drugs. J. Biol. Chem. 273, 21519–21525.

Sundaram, M., Yao, S.Y., Ingram, J.C., Berry, Z.A., Abidi, F., Cass, C.E., Baldwin, S.A., Young, J.D., 2001a. Topology of a human equilibrative, nitrobenzylthioinosine (NBMPR)-sensitive nucleoside transporter (hENT1) implicated in the cellular uptake of adenosine and anti-cancer drugs. J. Biol. Chem. 276, 45270–45275.

Sundaram, M., Yao, S.Y., Ng, A.M., Cass, C.E., Baldwin, S.A., Young,

J.D., 2001b. Equilibrative nucleoside transporters: mapping regions of interaction for the substrate analogue nitrobenzylthioinosine (NBMPR) using rat chimeric proteins. Biochemistry 40, 8146–8151.

Tabrizchi, R., Bedi, S., 2001. Pharmacology of adenosine receptors in the vasculature. Pharmacol. Ther. 91, 133–147.

Van Belle, H., 1993. Nucleoside transport inhibition: a therapeutic approach to cardioprotection via adenosine? Cardiovasc. Res. 27, 68–76.

Van Belle, H., 1995. Myocardial protection by nucleoside transport inhibition. Transplant. Proc. 27, 2804–2805.

Vickers, M.F., Mani, R.S., Sundaram, M., Hogue, D.L., Young, J.D., Baldwin, S.A., Cass, C.E., 1999. Functional production and reconstitution of the human equilibrative nucleoside transporter (hENT1) in *Saccharomyces cerevisiae*. Interaction of inhibitors of nucleoside transport with recombinant hENT1 and a glycosylation-defective derivative (hENT1/N48Q). Biochem. J. 339, 21–32.

Visser, F., Vickers, M.F., Ng, A.M., Baldwin, S.A., Young, J.D., Cass, C.E., 2002. Mutation of residue 33 of human equilibrative nucleoside transporters 1 and 2 alters sensitivity to inhibition of transport by dilazep and dipyridamole. J. Biol. Chem. 277, 395–401.

Vyas, S., Ahmadi, B., Hammond, J.R., 2002. Complex effects of sulfhydryl reagents on ligand interactions with nucleoside transporters: evidence for multiple populations of ENT1 transporters with differential sensitivities to *N*-ethylmaleimide. Arch. Biochem. Biophys. 403, 92–102.

Ward, J.L., Sherali, A., Mo, Z.P., Tse, C.M., 2000. Kinetic and pharmacological properties of cloned human equilibrative nucleoside transporters, ENT1 and ENT2, stably expressed in nucleoside transporter-deficient PK15 cells. ENT2 exhibits a low affinity for guanosine and cytidine but a high affinity for inosine. J. Biol. Chem. 275, 8375–8381.

Williams, E.F., Barker, P.H., Clanachan, A.S., 1984. Nucleoside transport in heart: species differences in nitrobenzylthioinosine binding, adenosine accumulation, and drug-induced potentiation of adenosine action. Can. J. Physiol. Pharm. 62, 31–37.

Yang, X., Zhu, Q., Claydon, M.A., Hicks Jr., G.L., Wang, T., 1994. Enhanced functional preservation of cold-stored rat heart by a nucleoside transport inhibitor. Transplantation 58, 28–34.

Yao, S.Y., Ng, A.M., Muzyka, W.R., Griffiths, M., Cass, C.E., Baldwin, S.A., Young, J.D., 1997. Molecular cloning and functional characterization of nitrobenzylthioinosine (NBMPR)-sensitive (es) and NBMPR-insensitive (ei) equilibrative nucleoside transporter proteins (rENT1 and rENT2) from rat tissues. J. Biol. Chem. 272, 28423–28430.

Yao, S.Y., Ng, A.M., Vickers, M.F., Sundaram, M., Cass, C.E., Baldwin, S.A., Young, J.D., 2002. Functional and molecular characterization of nucleobase transport by recombinant human and rat equilibrative nucleoside transporters 1 and 2. Chimeric constructs reveal a role for the ENT2 helix 5-6 region in nucleobase translocation. J. Biol. Chem. 277, 24938–24948.